UNCERTAINTIES OF ANTIPROTON AND POSITRON SPECTRA FROM B/C DATA AND MSUGRA CONTRIBUTIONS FOR CLUMPY HALOS

Andrea Lionetto [a], Aldo Morselli [a] and Vladimir Zdravković [b]

[a] *INFN, Sezione di Roma II, via della Ricerca Scientifica, Roma, Italy*

[b] *Dipartimento di Fisica, Università di Roma "Tor Vergata", via della Ricerca Scientifica, Roma, Italy*

Abstract

We have studied the variation of e^+ and $\bar{p}$ top of the atmosphere spectra due to the parameters uncertainties of the Milky Way geometry, propagation models and cross sections. We have used the B/C data and Galprop code for propagation analysis. We have also derived the uncertainty bands for subFe/Fe ratio, H and He. Finally we have considered a neutralino induced component in the mSUGRA framework. We conclude that even in the case of diffusion convection model for the standard propagation, where secondary spectra gives a good fit of the data, SUSY contribution can not be excluded up to now due to the overall uncertainties.

1 Production and Propagation of Cosmic Rays in the Milky Way

We have chosen Galprop [1] as a public code for the treatment of propagation of all cosmic rays (CR) together. Our scope has been to determine the total uncertainties in the calculation of e^+ and $\bar{p}$ top of the atmosphere spectra due to the uncertainties of geometrical and propagation parameters and cross sections. Here we give very short description of processes included in propagation equation:

$$\begin{aligned}\frac{\partial\psi(\mathbf{r},p,t)}{\partial t} &= q(\mathbf{r},p) + \nabla\cdot(D_{xx}\nabla\psi - \mathbf{V}_c\psi) + \frac{d}{dp}\,p^2 D_{pp}\frac{d}{dp}\,\frac{1}{p^2}\,\psi \\ &- \frac{\partial}{\partial p}\left[\dot{p}\psi - \frac{p}{3}\,(\nabla\cdot\mathbf{V}_c)\psi\right] - \frac{1}{\tau_f}\psi - \frac{1}{\tau_r}\psi\,. \qquad (1)\end{aligned}$$

where $\psi(\mathbf{r},p,t)$ is total phase space density. This equation is valid for all the types of particles. Isotropic diffusion is defined by the coefficient that depends

from rigidity (momentum per unit of charge, $\rho = \frac{p}{Z}$) $D_{xx} = \beta D_0(\rho/\rho_0)^\delta$, inspired by Kolmogorov spectrum ($\delta = 1/3$) of weak magnetohydrodynamic turbulence [6]. In some models we have used a break in the index δ at some rigidity ρ_0, with a value $\delta_1 = 0$ below the reference rigidity ρ_0. The convection velocity field $\mathbf{V}_c$, that corresponds to the Galactic wind, has a cylindrical symmetry and its z-component is the only one different from zero. It increases linearly with the distance z from the galactic plane , in agreement with magnetohydrodynamical models [3]. Reacceleration is determined by the diffusion coefficient for the impulse space D_{pp} that is a function of the corresponding configuration space diffusion coefficient and of the Alfven velocity V_A in the framework of quasi-linear MHD theory [2]. Of course, Alfven velocity and convection velocity gradient in Milky Way for reacceleration and convection terms are unknown parameters of propagation (there are no other sources of information from which we could extract them, except the spectra of cosmic rays) and their possible range will be constrained by the analysis of fits of suitable data. The same procedure is valid for constraining the height of the galactic halo and the other unknown parameters. This will be analyzed further in order to obtain all the possible spectra of antiprotons and positrons using the sets of the constrained parameters. Injected spectra of all primary nuclei are power law in impulse $dq(p)/dp \propto p^{-\gamma}$. This power law approximation has been shown to be allowed in the framework of diffusive shock acceleration models, as well as in model with a small break in the injection indexes γ [4, 8, 7]. Source term $q(\mathbf{r}, p)$ for secondaries contains cross sections for their production from progenitors on H and He targets. The last two terms in equation 1 are loss terms with characteristic times for fragmentation and radioactive decay. Propagation equation is solved numerically, using the Crank-Nicholson algorithm.

The heliospheric modulation in the vicinity of the Earth has to be taken in account. We have used a model in which transport equation (that describes diffusion processes in the heliosphere and includes effects of heliospheric magnetic field and solar wind) is solved in the force field approximation [9]. In this case solar modulation is a function of just a single parameter that describes the strength of the modulation. All the dynamical processes are simulated with relatively simple changing of the interstellar spectra during the propagation inside the heliosphere, described by the formula

$$\frac{\Phi^{toa}(E^{toa})}{\Phi^{is}(E^{is})} = (\frac{p^{toa}}{p^{is}})^2, \tag{2}$$

$$E^{is} - E^{toa} = |Ze|\phi \tag{3}$$

where E and p are energies and impulses of the interstellar and top of the atmosphere fluxes and ϕ is the unique parameter that determines the solar modulation.

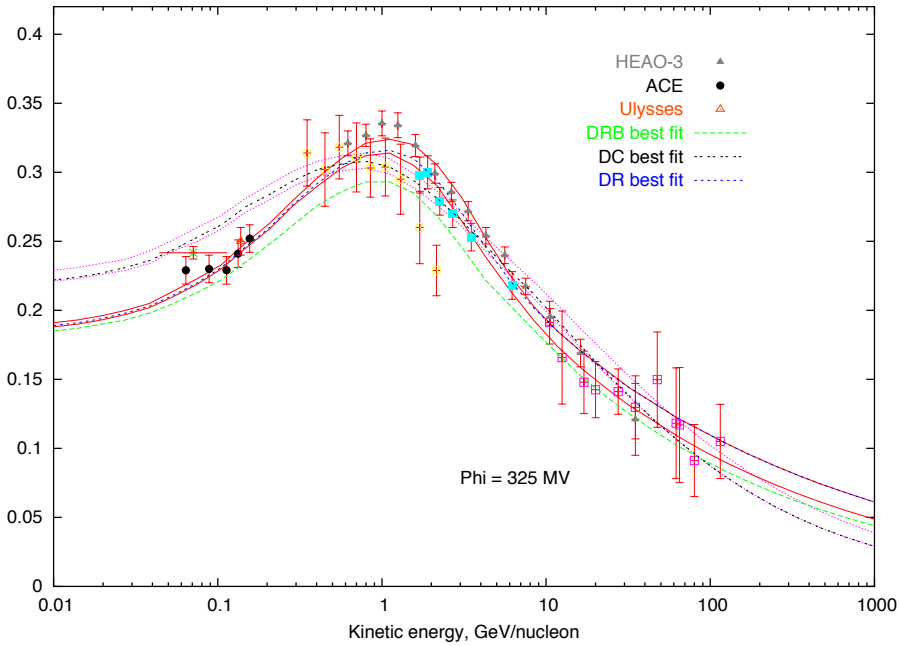

Figure 1: Enveloping curves of all the good fits of B/C data for DR and DC model with their best fits inside and the best fit for DRB model. For the complete list of data see [13].

2 Uncertainties of CR Spectra

We were treating the two extreme cases of propagation models: the first that uses diffusion and reacceleration (DR) and the second that contains diffusion and convection (DC) [5]. Many parameters in the propagation equation are free and must be constrained by experimental data. Secondary to primary CR ratios are the most sensitive quantities on variation of the propagation parameters. The most accurately measured parameter is boron to carbon ratio (B/C). We have used a standard χ^2 test:

$$\chi^2 = \sum_n \frac{1}{(\sigma_n^{B/C_{exp}})^2} (\Phi_n^{B/C_{exp}} - \Phi_n^{B/C_{teo}})^2 \tag{4}$$

For DR model we have required reduced χ^2 less than 2 for the fit of the experimental data [13] (fig. 1). We take the data with relatively small solar modulation between 325 MV and 600 MV where the force field approximation is better justified than for high modulation parameters. The allowed ranges of all parameters are given in table 1. Using them we have found the enveloping curves of all the e^+ and $\bar{p}$ spectra that present upper and lower bounds of uncertainty band. For

Table 1: Allowed values for DR model propagation parameters.

par./val.	$z[kpc]$	$D_0[cm^2s^{-1}]$	δ	γ	$v_A[kms^{-1}]$
minimal	3.0	$5.2\ 10^{28}$	0.25	2.35	22
best fit	4.0	$5.8\ 10^{28}$	0.29	2.47	26
maximal	5.0	$6.7\ 10^{28}$	0.36	2.52	35

Table 2: Allowed values for the propagation parameters for DC model.

par./val.	$z[kpc]$	$D_0[\frac{cm^2}{s}]$	δ_2	$\frac{dV_C}{dz}[\frac{km}{skpc}]$	γ_1	γ_2
minimal	3.0	$2.3\ 10^{28}$	0.48	5.0	2.42	2.14
best fit	4.0	$2.5\ 10^{28}$	0.55	6.0	2.48	2.20
maximal	5.0	$2.7\ 10^{28}$	0.62	7.0	2.50	2.22

e^+ relative uncertainty is varying from 30% under 1 GeV to 15% around 10 GeV (fig. 2, left) while for $\bar{p}$ is from about 10% up to 15%. For better visibility all the black and white figures that contain positron and antiproton data will contain just the part of the experimental data chosen to cover maximally all the energy range, while all the data are presented on the color figures. All data are taken from references [14, 15].

For DC model (fig. 1) we have taken all the reduced χ^2 values less than 2.8 for the variation of D_0, diffusion indexes δ_1, below, and δ_2, above the reference rigidity $\rho_0 = 4$ GV, z, V_c and injection index for primary nuclei γ_1 below the reference rigidity $\rho_0^\gamma = 20$ GV and γ_2 above it. Positive variations around $\delta_1 = 0$ gave unsatisfactory fit. In order to take the smallest possible break of this index we have decided not to take negative δ_1 values. Allowed values for the propagation parameters can be found in table 2. The same analysis as for DR model gives relative e^+ error between 20% above the maximum and 30% below it (fig. 2, left) while for $\bar{p}$ is about 20% around 20 MeV, 17% around the maximum and 25% around 20 GeV (fig. 2, right). We calculated PAMELA expectations for e^+ (fig. 4) and $\bar{p}$ (fig. 5) (parameters of the best B/C fit) using its geometrical factor and detector characteristics [10] during the three years mission in which it will measure with high statistics various cosmic rays spectra. We have found also spectra that correspond to the parameters of the best fit of B/C data for subFe/Fe ratio (another important ratio for testing the parameters of the propagation models, fig. 3), protons, He and e^- as well as corresponding uncertainties. For DC model fits are good, while DR overestimates p, He and e^-.

We have considered also the DR model with a break in the injection index for the primary nuclei spectra taken at rigidity of 10 GV [5, 7]. We determined allowed values of the propagation parameters (table 3) demanding the same χ^2 as for DR model (fig. 1). The positron and antiproton uncertainties are presented in

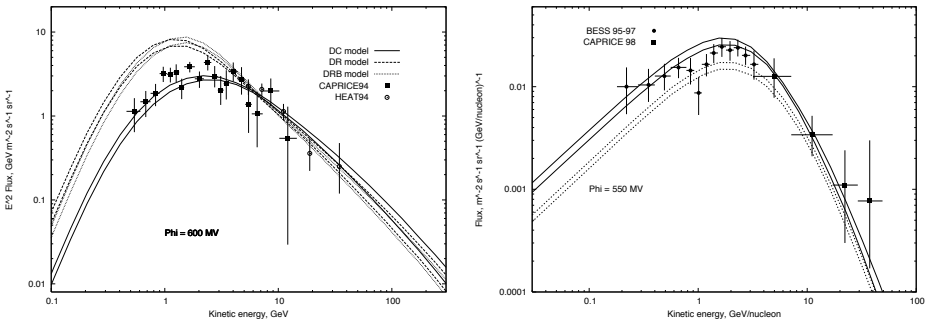

Figure 2: Upper and lower bounds of positron (left) and antiproton (right) spectra due to uncertainties of the propagation parameters for DC, DR DRB model and DC and DRB model respectively. Experimental data are taken from [15, 14].

Table 3: Allowed values for the propagation parameters for DR model with the break.

par./val.	$z[kpc]$	$D_0[\frac{cm^2}{s}]$	δ	γ_1	γ_2	$v_A[\frac{km}{s}]$
minimal	3.5	$5.9\ 10^{28}$	0.28	1.88	2.36	25
best fit	4.0	$6.1\ 10^{28}$	0.34	1.92	2.42	32
maximal	4.5	$6.3\ 10^{28}$	0.36	2.02	2.50	33

fig. 2. Even if e^+ are fitted a little bit better at low energies and also primaries are fitted better, all of them remain overestimated while $\bar{p}$ spectra remain practically unchanged. For this reason on fig. 5 and fig. 2, on the right, we refer just the DRB case.

We have also seen how the obtained antiproton spectra change on variation of the most important antiproton production cross sections. Those are reactions that include all the types of hydrogen and helium. Antiprotons are created in the interactions of primary cosmic rays (protons and other nuclei) of sufficiently high energies with interstellar gas. Dominant processes are interactions of high energy primary protons with hydrogen, for example $p + p \rightarrow p + p + p + \bar{p}$. Parameterization of this cross sections used in our version of Galprop code is given by Tan and Ng [11]. Other used cross sections, those of primary protons with other nuclei, are studied in reference [12]. From these, the most important are those that involve helium and they contribute less than 20% of the total production of all the antiprotons. All the heavier nuclei together give just a few percents of the total production. Simultaneous settings of all the production cross sections to the maximum/minimum rise/lower the upper/lower parameter uncertainty bounds. Errors obtained in this way give contributions to the total uncertainties varying from 20% up to 25% in the case of DR model and, almost the same, from 20% up to 24% for

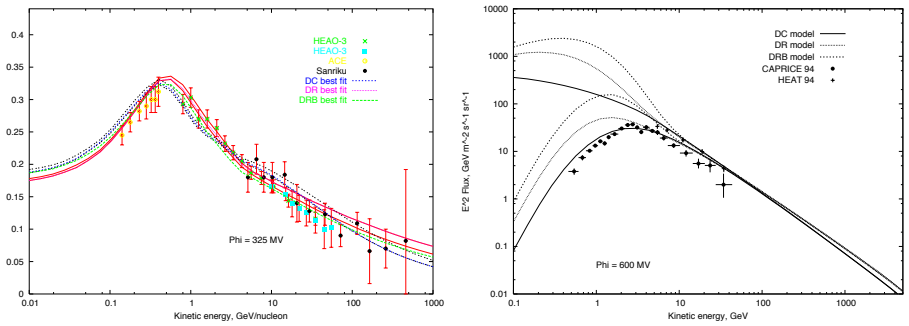

Figure 3: Left: Ratios (Sc+Ti+V)/Fe that correspond to the parameters of propagation for DC, DR and DRB model that gave the best fits of B/C data. The upper and the lower limits of all the graphics obtained with the parameters that give good fits of boron to carbon ratio are given for DC and DR model. Experimental data are taken from[17]. Right: Top of the atmosphere spectra of e^- that correspond to the parameters of the best B/C fit for DC, DR and DRB model (lower curves) and local interstellar spectra (upper curves). Experimental data are taken from [15].

DC model, depending of the energy range of the spectra. Non production cross sections, the so called tertiary component, correspond to inelastically scattered secondaries $\bar{p} + X \rightarrow \bar{p} + \tilde{X}$. Those processes tend to bring down the energies of the antiprotons of relatively high energies, flattening like that the spectra. But, even if their uncertainty is relatively big, this does not give relevant change of the spectra because tertiary contribution is very small.

Changing of another exactly unknown quantity, He/H ratio, in a reasonable range from 0.08 to 0.11 gives a relatively small contribution, that vary from 3% - 7% depending of the energy, for both e^+ and $\bar{p}$ uncertainty, and for both of the models. Total uncertainties of e^+ and $\bar{p}$ are presented at fig. 4 and fig. 5 respectively. They vary from 35% up to 55% for antiprotons and from 20% up to 40% for positrons roughly for both of the models in the current experimental data energy range.

3 Antiproton Flux from Neutralino Annihilations

In this section we take into account the possibility of a neutralino induced component in the $\bar{p}$ flux. Our analysis is performed in the well known mSUGRA framework [18] with the usual gaugino mass universality at the grand unification scale M_{GUT}. The five input parameters are defined as follows:

$$m_{1/2}, \;\; m_0, \;\; sign(\mu), \;\; A_0 \;\; \text{and} \;\; \tan\beta \, ,$$

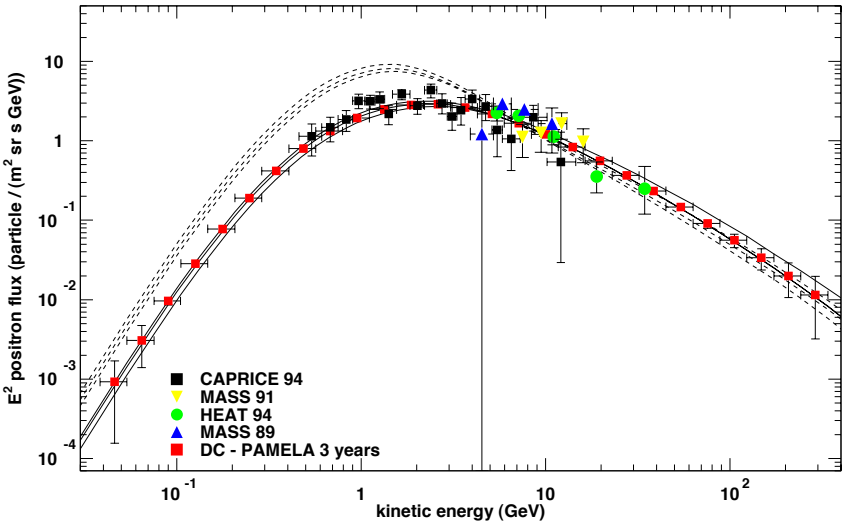

Figure 4: Total uncertainties of e^+ fluxes and spectra that correspond to the parameters of the best B/C fit for DC (solid lines around the best fit) and DRB model (dashed lines around the best fit). Experimental data (from [15]) vs. PAMELA expectations for DC model.

where m_0 is the common scalar mass, $m_{1/2}$ is the common gaugino mass and A_0 is the proportionality factor between the supersymmetry breaking trilinear couplings and the Yukawa couplings. $\tan\beta$ denotes the ratio of the vacuum expectation values of the two neutral components of the SU(2) Higgs doublet, while the Higgs mixing μ is determined (up to a sign) by imposing the Electro-Weak Symmetry Breaking (EWSB) conditions at the weak scale. The parameters at the weak energy scale are determined by the evolution of those at the unification scale, according to the renormalization group equations (RGEs) [19]. For this purpose, we have made use of the ISASUGRA RGE package in the ISAJET 7.64 software [20]. After fixing the five mSUGRA parameters at the unification scale, we extract from the ISASUGRA output the weak-scale supersymmetric mass spectrum and the relative mixings. Cases in which the lightest neutralino is not the lightest supersymmetric particle or there is no radiative EWSB are disregarded. We have assumed a small clump scenario [21] for the dark matter halo in our galaxy. By hypothesis the clump is a spherical symmetric compact object with mass M_{cl} and density profile $\rho_{cl}\left(\vec{r}_{cl}\right)$. We denote with f the dark matter fraction concentrated in clumps and we introduce the dimensionless parameter d

$$d = \frac{1}{\rho_0} \frac{\int d^3 r_{\rm cl} \left[\rho_{\rm cl}\left(\vec{r}_{\rm cl}\right)\right]^2}{\int d^3 r_{\rm cl} \rho_{\rm cl}\left(\vec{r}_{\rm cl}\right)} \tag{5}$$

that gives the overdensity due to a clump with respect to the local halo density

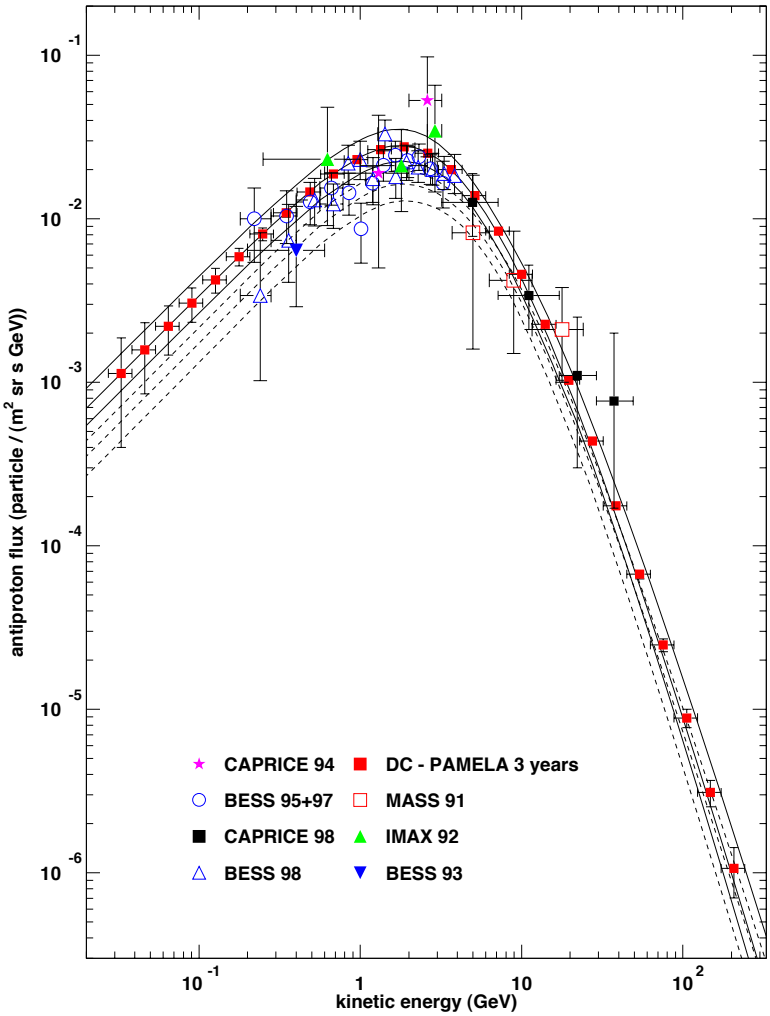

Figure 5: Total uncertainty of $\bar{p}$ fluxes and spectra that correspond to the parameters of the best B/C fit for DC (solid lines) and DRB model (dashed lines). Experimental data (from [14]) vs. PAMELA expectations for DC and DRB model.

$\rho_0 = \rho(r_0)$, where r_0 is our distance from the Galactic center. In a smooth halo scenario the total neutralino induced $\bar{p}$ flux calculated for $r = r_o$ is given by [22]

$$\Phi_{\bar{p}}(r_0, T) \equiv (\sigma_{\rm ann} v) \sum_f \frac{dN^f}{dT} B^f \left(\frac{\rho_0}{m_{\tilde{\chi}}}\right)^2 C_{\rm prop}(T) \, . \tag{6}$$

where T is the $\bar{p}$ kinetic energy, $\sigma_{\rm ann} v$ is the total annihilation cross section times the relative velocity, m_χ is the neutralino mass, B^f and dN^f/dT, respectively, the branching ratio and the number of $\bar{p}$ produced in each annihilation channel f per unit energy and $C_{\rm prop}(T)$ is a function entirely determined by the propagation model.

In the presence of many small clumps the $\bar{p}$ flux is given by

$$\Phi_{\bar{p}}^{\rm clumpy}(r_0, T) = fd \cdot \Phi_{\bar{p}}(r_0, T) \tag{7}$$

For the smooth profile we have assumed a Navarro, Frenck and White profile (NFW) [23].

The primary contribution to the $\bar{p}$ flux has been computed using the public code DarkSUSY [24]. We have modified the $\bar{p}$ propagation in order to be consistent with the DC model as implemented in Galprop. We assumed diffusion coefficient spectra used in Galprop with our best fit values for the diffusion constants D_0 and δ. In DarkSUSY the convection velocity field is constant in the upper and lower Galactic hemispheres (with opposite signs, and so it suffers unnatural discontinuity in the Galactic plane) while Galprop uses magnetohydrodynamically induced model in which component of velocity field along the Galactic latitude (the only one different from zero) increases linearly with the galactic latitude [3]. We have assumed an averaged convection velocity calculated from the Galactic plane up to the Galactic halo height z.

We present here four different susy contribution to the $\bar{p}$ flux for different neutralino masses (obtained from a particular choice of mSUGRA parameters) and different clumpiness factor fd. Higher neutralino masses improve high energy data fit but only with the increase of the clumpiness factor because of the dependence from the inverse neutralino mass squared m_χ in the $\bar{p}$ flux formula (5). We remark that for those models we have not computed the neutralino relic density.

4 Conclusions

For e^+ in DR model, even when the uncertainties are included, the curve of the minimal e^+ production still remains above the experimental results. Breaking the primary spectra gently improves just the low energy part of the spectra below the maximum, but even the minimal predictions still remain bigger than the experimental results around the maximum as well as below it. On the other side, this slightly changes the best B/C fit (fig. 1). This is also not sufficient to match protons and helium, that are still overestimated. In the end, e^- remain largely overproduced at low energies, even more than without the break. Uncertainty

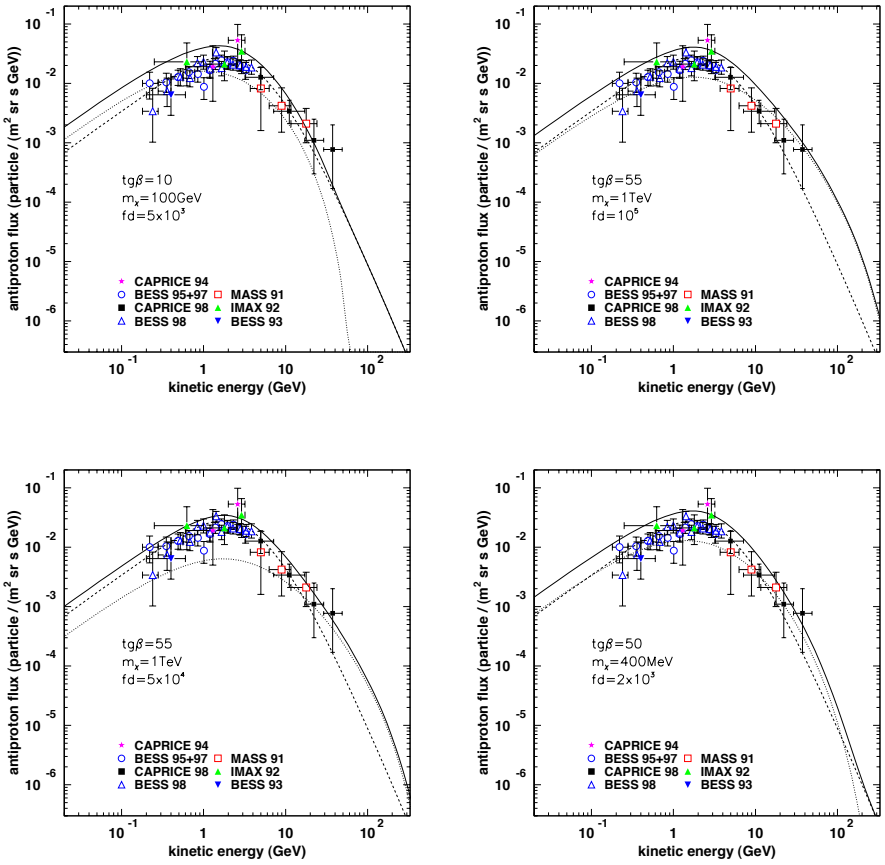

Figure 6: Different susy contribution to the total $\bar{p}$ flux with the DC model background. The dashed lines correspond to the background contribution, the punctuated lines correspond to the neutralino induced contribution while the solid lines correspond to total contribution

bands of $\bar{p}$ in DR models touch the experimental data from below. In this case the fit can be improved easily with any primary component that is coming from eventual neutralino annihilation or some other exotic contribution. For DC model all the results are in good agreement with the data, with only some problems with B/C data.

As a possibility for the future considerations we would like to emphasize that it is natural to expect models that include both of the processes – convection and reacceleration, and this perhaps can be a key to solve simultaneously problems with

positrons, electrons and B/C. But, we have not yet found such a kind of models. In any case, further measurements of $\bar{p}$ and e^+ spectra, primary to secondary CR ratios and Solar effects on them, as well as the precise determination of important nuclear cross sections seem to be crucial for answering the question of the models quality.

In the framework of DC model exotic contributions remain possible at high energies (E > 20 GeV), and also they are not excluded at lower energies due to the relatively large uncertainties (if the Standard Model productions are smaller than the best fits). In the case of DR model background it is possible to improve the $\bar{p}$ data fit adding a neutralino induced component for a large part of the parameter space. Finally we have shown how a possible neutralino induced component in a clumpy halo scenario could give a contribution to the total $\bar{p}$ flux, in the case of DC model background.

References

[1] Strong, A. W., Moskalenko, I. V., 1998, ApJ, 509, 212

[2] Fermi, E., 1949, Phys. Rev., 75, 1169; Seo, E. S., Ptuskin, V. S., 1994, ApJ, 431, 705; Berezinskii, V. S., Bulanov, S. V., Dogiel, V. A., Ginzburg, V. L., Ptuskin, V. S. 1990, Astrophysics of Cosmic Rays (North Holland, Amsterdam)

[3] Zirakashvili, V. N., Breitschwerdt, D., Ptuskin, V. S., Volk, H. J., 1996, A&A, 311, 113

[4] Blandford, R. D. & Ostriker, J. P. (1980) ApJ, 237, 793

[5] Moskalenko, I. V., Strong, A. W., Ormes, J. F., Potgieter, M. S., 2002, ApJ, 565, 280

[6] U. Heinbach, M. Simon, 1995, ApJ, 441, 209-221

[7] Ellison, D. C., Slane, P., Gaensler, B. M., astro-ph/0106257

[8] Strong, A. W., Mattox, J. R., 1996, 308, L21

[9] Gleeson, L. J., Axford, W. I., 1996, ApJ, 154, 1011; Perko, J. S., 1987, A&A, 184, 119

[10] O. Adriani et al., Nucl. Inst. and Meth. in Phys. Research A, 478 (2002) 114-118; P. Papini, PAMELA Simulations; Picozza, P., Morselli A., 2003. J. Phys. G: Nucl. Part. Phys., 29, 903-911

[11] Tan, L. C., Ng, L. K., 1983, J. Phys. G, 9, 227 and 1289

[12] Gaisser, T. K., Schaefer, R. K., 1992, ApJ, 394, 174

[13] ACE: A. J. Davis at al., 2000, AIP Conf. Proc. 528, ed. R. A. Mewaldtet al. (AIP, New York); Ulysses: Du Vernois, M. A. at al., 1996, A&A, 316, 555; Voyager: A. Lukasiak et al., 1999, Proc. 26th Int. Cosmic-Ray Conf. (Salt Lake City), 3, 41; HEAO 3: Engelmann, J. J. et al., 1990, A&A, 233, 96; Caldwell, J. H., Meyer, P., 1977, Proc. 15th Int. Cosmic-Ray Conf. (Plovdiv), 1, 243; Dwyer, R. 1978, ApJ, 224, 691; Juliusson, E. 1974, ApJ, 191, 331; Simon, M., et al. 1980, ApJ, 239, 712

[14] CAPRICE '98: M. Boezio et al., Astrophys. Journ. 561 (2001) 787; BESS '95 and '97: S. Orito et al., Phys. Rev. Lett. 84 (2000) 1078; BESS '98: T. Maeno et al., Astroparticle Physics 16 (2001) 121-128; CAPRICE '94: M. Boezio et al., Astrophys. Journ. 487 (1997) 415; BESS '93: A. Moiseev et al., Astrophys. Journ. 474 (1997) 479; IMAX '92: J.W. Mitchell et al., Phys. Rev. Lett. 76 (1996) 3057; MASS '91: G. Basini et al., Proc. 26th ICRC (1999) OG.1.1.21

[15] CAPRICE '94: Boezio M. et al. 2000, ApJ 532, 653; HEAT '94: Barwick S. et al. 1997, ApJ 498, 779; MASS 91: C. Grimani et al. 2002, A&A 392, 287-294; MASS '89: R. L. Golden 1994, ApJ 436, 769-775

[16] Proton and helium spectra: CAPRICE '98: M. Boezio et al., Astroparticle Physics, 19, (2003) 583-604; CAPRICE '94: M. Boezio et al., ApJ, 518:457-472 (1999); BESS: T. Sanuki et al. (2000) ApJ, 545, 1135

[17] subFe/Fe ratio: ACE: A. J. Davis et al. (2000) On the low energy decrease in Galactic cosmic ray Proc ACE-2000 Symp., editors R. A. Mewald et al. (NY: AIP), AIP Conf. Proc. 528, 421-424, 2000; HEAO-3: W. R. Binns et al., ApJ 324, 1106-1117, 1988 and J. J. Engelmann et al., A&A 233, 96-111, 1990; Sanriku experiment: M. Hareyama et al., 26th ICRC (Salt Lake City) 3, 105-108, 1999

[18] L. J. Hall, J. Lykken and S. Weinberg, Phys. Rev. D **27** (1983) 2359.

[19] A. Cesarini, F. Fucito, A. Lionetto, A. Morselli and P. Ullio, Astropart. Phys. **21** (2004) 267 [arXiv:astro-ph/0305075].

[20] H. Baer, F. E. Paige, S. D. Protopopescu and X. Tata, hep-ph/0001086. The source code is available at ftp://ftp.phy.bnl.gov/pub/isajet

[21] L. Bergstrom, J. Edsjo, P. Gondolo and P. Ullio, Phys. Rev. D **59** (1999) 043506 [arXiv:astro-ph/9806072].

[22] L. Bergstrom, J. Edsjo and P. Ullio, arXiv:astro-ph/9902012.

[23] J.F. Navarro, C.S. Frenk, & S.D.M. White, ApJ, **462** (1996) 563.

[24] P. Gondolo, J. Edsjo, P. Ullio, L. Bergstrom, M. Schelke and E. A. Baltz, JCAP **0407** (2004) 008 [arXiv:astro-ph/0406204].